

New insights from electron spin polarization studies of surfaces

D. T. Pierce and R. J. Celotta

National Bureau of Standards, Washington, D.C. 20234

(Received 20 August 1982; accepted 4 October 1982)

Examples of recent investigations in several laboratories, where measurement of effects due to electron spin polarization provided new insight into surface phenomena, will be reviewed. The results to be discussed include the use of spin dependent electron scattering to determine the surface potential barrier, the magnetic critical behavior of a semi-infinite solid, and the low temperature surface magnetization. Examples from spin-polarized photoemission include studies of the nature of the resonant 6 eV satellite in Ni and of oxygen-induced magnetism in a Cr(100) surface. The use of angle-resolved spin-polarized inverse photoelectron spectroscopy to obtain information on spin dependent band structure of unoccupied states will also be described. The rapid growth of measurements involving electron spin polarization, where previously only electron energy or momentum was measured, is explained by the development of new experimental techniques like the GaAs spin-polarized electron source and advances in spin polarization detectors.

PACS numbers: 75.30. — m, 73.30. + y, 79.20.Kz, 79.60.Cn

I. INTRODUCTION

When electrons are used to investigate the structural, electronic, or magnetic properties of surfaces, a measurement is usually made of the number of electrons at a given energy or momentum, which result from a particular emission or scattering process. For many problems, new insights can be obtained if another parameter is considered, namely, the electron spin polarization. Spin dependent effects result from the spin orbit interaction, which is largest for surfaces containing high Z elements, and from the exchange interaction, which allows one to probe magnetic surfaces.

To illustrate the type of new information which can be gained from spin dependent studies, we present highlights of six investigations reported in the past year in the areas of spin dependent scattering¹ and spin-polarized photoemission²: (1) determination of the surface potential barrier of W(100)^{3,4}; (2) determination of the critical exponent of surface magnetization^{5,6}; (3) observation of the effect of the surface on the magnetization at low temperature⁷; (4) discovery of oxygen-induced magnetic order for Cr(100)⁸; (5) test of models for the resonant enhancement of the 6-eV Ni satellite⁹; and (6) measurement of the spin polarization of unoccupied states by angle-resolved spin-polarized inverse photoelectron spectroscopy.¹⁰

It must be recognized that this selection of illustrative examples is, of necessity, very limited and does not do justice to such other techniques as tunneling spectroscopy,¹¹ electron capture spectroscopy,¹² field emission,¹³ or secondary electron emission,^{14,15} all techniques in which spin dependent measurements have been very fruitful. For example, recent electron capture spectroscopy measurements¹² provided evidence for "local" ferromagnetic order above the Curie temperature of Ni. Recent results from secondary emission showed that low energy secondaries from a ferromagnet are highly polarized and may provide a means to measure magnetic microstructures with the spatial resolution of a scanning electron microscope.¹⁴

The surge in activity in electron spin polarization studies

of surfaces in the past few years has been due in large part to technical advances which have made new experiments possible. Spin-polarized electron sources¹⁶⁻¹⁹ using photoemission from negative electron affinity GaAs are capable of producing high current beams (comparable to conventional electron guns) with an approximately 40% spin polarization that can be easily reversed without affecting the beam intensity. There have been improvements in the traditional Mott spin analyzer and two new polarization detectors have been introduced, one based on spin dependent diffraction in LEED²⁰ and the other on the fact that the current absorbed when an electron beam hits a metal is spin dependent.²¹⁻²³

II. SURFACE POTENTIAL BARRIER OF W(100)

The shape of the potential barrier which acts on electrons near a metal surface is important in calculations of electron states and electron scattering at surfaces. Calculated LEED intensity curves of the fine structure near a beam emergence threshold are very sensitive to the model of the surface potential barrier which can thus be tested by comparing to experimental data in this region.²⁴ This fine structure, which appears as a characteristic Rydberg-like series of peaks converging on a beam emergence threshold, was originally described as a resonance effect.²⁵ Recently, Dietz *et al.*²⁶ and LeBosse *et al.*²⁷ have shown that the threshold features are more appropriately described as an interference between two beams.

Dietz *et al.* made high resolution threshold measurements for a Cu(100) surface to test the surface potential model shown in the inset of Fig. 1. Far from the surface the classical image potential $U = 1/2(z - z_0)$ is valid. Near the surface, the potential saturates; that is, it goes over to the inner potential $U = U_0$ rather than becoming infinite at z_0 . In describing the potential, z is positive into the metal, $z = 0$ is the position of the surface layer of atoms, and z_0 is the center of mass of the induced charge density. In their model, the asymptotic form is extended linearly to the surface where it has the value U_1 , and there drops abruptly to U_0 . They found that calcu-

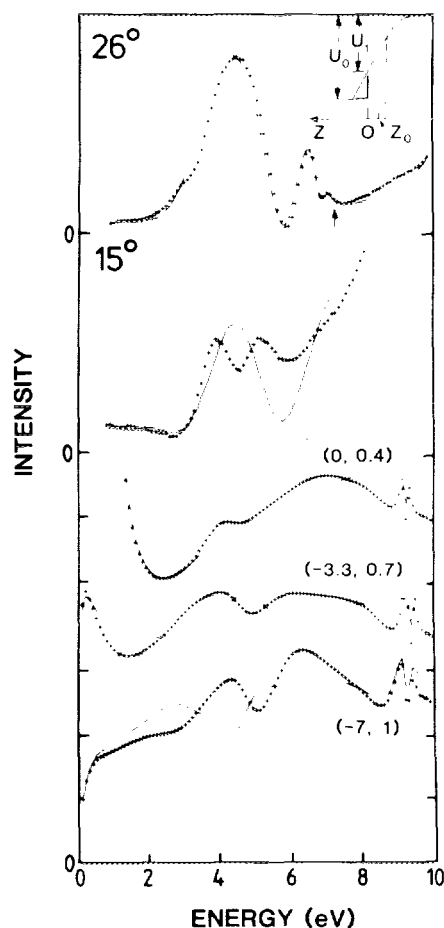


FIG. 1. The upper two curves show two measured (Ref. 29) reflected intensity curves for beams of up-spin (+) and down-spin (-) electrons at 26° and 15° angle of incidence. The lower three curves are the intensities at 15° calculated by Jennings and Jones (Ref. 3) for three different pairs of parameters (z_0, U_1) where z_0 is given in bohr and U_1 in Rydbergs. The curves are displaced vertically for clarity. The inset shows schematically the models of the surface potential discussed in the text.

lated curves fit the experimental data for a whole family of parameters (z_0, U_1).

In a recent analysis of the W(100) surface, Jennings and Jones^{3,4} used a barrier model like that of Dietz *et al.*,²⁶ except that it continued smoothly to U_0 without a discontinuity at the surface. They point out that such a one-dimensional saturated image barrier is approximate but it contains two critical features, the translation of the image plane and the barrier saturation. Using the high resolution (15 meV) data of Adnot and Carotte,²⁸ Jennings and Jones found three pairs of parameters (z_0, U_1) which gave calculated curves which reproduced the LEED data. Fortunately, the spin dependence of the threshold fine structure had also been measured,²⁹ in this case, at angles of incidence from 15° to 43°. The spin-polarized electron scattering data allowed Jennings and Jones to determine a *unique* set of parameters that describe the surface barrier potential of W(100).

Two representative experimental-polarized LEED (PLEED) curves for specular scattering from W(100) near the (01) beam emergence threshold are shown in the upper part of Fig. 1. The 130 meV resolution of the GaAs-polarized electron source is sufficient to observe some of the char-

acteristic Rydberg-like structure converging on the threshold marked by the arrow. The spin dependence is due to the spin-orbit interaction in the scattering of the spin-polarized incident beam from atoms in the substrate. A very strong spin dependence can be seen in the 15° data where the spin up curve shows a double peak and the spin down curve a single peak. This curious double peak in the spin up curve at 15° could be explained⁴ as the interaction of interference fine structure with Bragg peak without invoking additional mechanisms such as the double resonance suggested by Malmström and Rundgren.³⁰ The calculated curves at $\alpha = 15^\circ$ for the three pairs of parameters (z_0, U_1) are shown at the bottom of the figure. A spin dependent calculation including the saturated image barrier ($-3.3, 0.7$) reproduces the PLEED experimental peak structure. Thus, the image plane is found to be 3.3 bohr outside the surface layer, and the potential at the surface layer, was found to have value 70% of the bulk value.

III. SURFACE MAGNETIC CRITICAL BEHAVIOR OF Ni(100) AND Ni(110)

Alvarado and co-workers^{5,6} have shown that the magnetic critical behavior of well-characterized surfaces can be determined by spin-polarized low energy electron scattering. In a series of beautiful experiments, using a polarized beam from a GaAs source,¹⁹ they measured the critical exponent β_1 of the surface magnetization for Ni(100) and Ni(110) surfaces.

Because of the exchange interaction between the incident electron spin and the magnetic surface, the scattered intensity I_s for incident spin polarization parallel to the majority spins in the surface (antiparallel to the magnetization) is different from the scattered intensity I_i when the spin polarization of the incident beam is in the opposite direction. Experimentally, one measures the normalized scattering asymmetry A ,

$$A = \frac{1}{|P_0|} \frac{I_{\uparrow} - I_{\downarrow}}{I_{\uparrow} + I_{\downarrow}},$$

for scattering an incident beam of polarization P_0 .

Electrons incident on a single crystal may be diffracted and multiply scattered so that, in general, A is not related to the surface magnetization M_s in a simple way. All that can be said from symmetry is that A must be proportional to an odd power of M_s . However, near the critical temperature, it can further be shown³¹ that A is directly proportional to M_s . This assumes that the electron probing depth is less than the coherence length of the surface magnetic disturbance which is indeed the case.⁶

The critical exponent can therefore be determined from the measured asymmetry data by fitting the function

$$A(T) \propto M_s(T) \propto (1 - T/T_c)^{\beta_1}.$$

The high precision data of Alvarado *et al.*⁶ for the specular scattering of a 49-eV beam from a Ni(110) surface at an angle of incidence of 15° are shown in Fig. 2. The value of β_1 determined from the slope was 0.769 ± 0.02 . Alvarado *et al.* measured β_1 for three beams on Ni(100) and two beams on Ni(110) to determine the average values 0.81 ± 0.02 and 0.79 ± 0.02 , respectively. The temperature range in each

case was $0.002 \leq 1 - T/T_c \leq 0.1$.

The theoretical values of β_1 , which can be determined by direct calculation or from scaling relations, range from 0.81 to 0.88 for the Heisenberg model, 0.79 to 0.84 for the XY model, and 0.78 to 0.82 for the Ising model.⁶ The experimental values, surprisingly, are somewhat less than the range of predictions of the Heisenberg model. The stated experimental uncertainty at this point is smaller than the uncertainty in the calculations, suggesting the need for more theoretical work. The agreement within experimental uncertainty of β_1 for the (100) and (110) surfaces demonstrates another point.⁶ Since the outer layer of Ni(110) is contracted by 5%–8% and that of Ni(100) by less than 3% if at all, it was possible to test whether the larger short range magnetic anisotropy of the (110) surface affects β_1 ; within experimental uncertainty no difference was found.

IV. SURFACE CONTRIBUTION TO THE MAGNETIZATION TEMPERATURE DEPENDENCE

The ferromagnetic metallic glass $\text{Ni}_{40}\text{Fe}_{40}\text{B}_{20}$ has been studied by spin-polarized low energy electron scattering,^{7,21} and a number of interesting effects were revealed in measurements of the spin dependent asymmetry of the elastic scattering, inelastic scattering, and absorbed current. We focus here on the temperature dependence of the elastic scattering asymmetry. In contrast to scattering from a single crystal where well-collimated diffracted beams dominate, the scattering from an amorphous ferromagnet is diffuse. It was shown⁷ that in the backscattering direction (scattering angle of 166°) the contribution of multiple scattering to the intensity was less than 30%. Under these conditions the scattering is atomlike and affords us the opportunity to study the spin dependence of the scattering from single magnetic atoms in a metallic environment. Moreover, since multiple scattering is small, we have $A \propto M_s$ to a good approximation at all temperatures. Thus, a ferromagnetic glass is an ideal sample for temperature dependent studies.

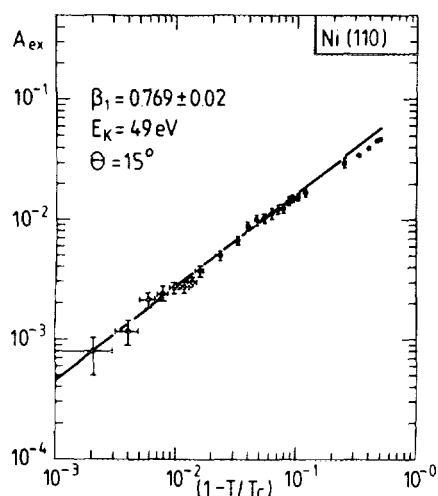


FIG. 2. The slope of the log-log plot of the scattering asymmetry for Ni(110) vs reduced temperature gives β_1 , the critical exponent of the surface magnetization. From Alvarado *et al.* (Ref. 6).

In 1967, Mills and Maradudin³² calculated the temperature dependence of the magnetization at the surface. They predicted that it should decrease with the same power law as the bulk

$$M_s(T)/M_s(0) = 1 - B_s T^{3/2} + \dots$$

but that the coefficient B_s should be twice as large as the corresponding bulk coefficient B_b . The enhanced spin deviation near the surface should also contribute to the specific heat, but this has not been possible to detect experimentally. It remained a challenge to experimentalists to test the predictions of Mills and Maradudin. This was recently accomplished by the measurement of the surface magnetization using polarized electron scattering.

The spin dependent asymmetry was measured for $T < 0.5 T_c$, in the regime of long wavelength magnons, and plotted against the bulk magnetization at each temperature. A straight line resulted, confirming that M_s and M_b decrease with the same power law. When the relative surface and bulk magnetization are displayed as functions of temperature, as in Fig. 3, M_s is seen to decrease faster than M_b . The dashed line on the figure represents a $T^{3/2}$ variation which was extended to $T = 0$. The coefficient B_s , which is responsible for the more rapid decrease of M_s , was found to be three times B_b . This is a lower limit since the electrons probe some of the bulk region. Thus, the surface magnetization decreases more rapidly than was predicted theoretically. The other prediction of Mills and Maradudin, namely, that $M_s \propto M_b$, was confirmed by these measurements.

V. OXYGEN-INDUCED MAGNETIC ORDER IN Cr(100)

Until recently, spin-polarized photoemission investigations have consisted of polarized photoyield measurements, that is, measurements of the spin polarization of all electrons photoemitted at a given photon energy. Measurements performed right at threshold are of course "energy-resolved" and by virtue of escape cone effects, angle-resolved. In spite of the limitations of such measurements, they have yielded a wealth of information.² A recent example is the discovery that the magnetic order of the Cr(100) surface changes from

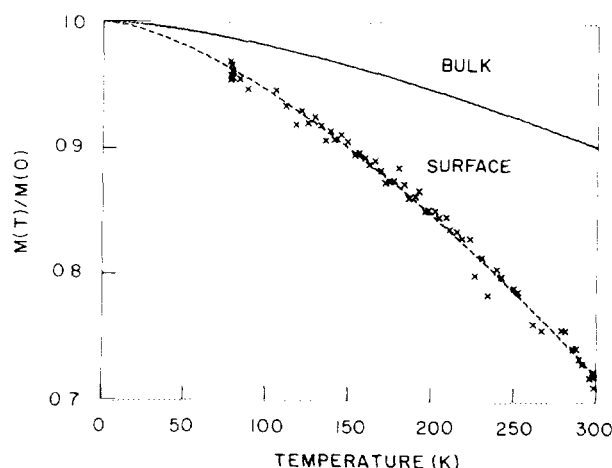


FIG. 3. The temperature dependence of the surface magnetization is found (Ref. 7) to decrease faster than that of the bulk.

antiferromagnetic to ferromagnetic on incorporation of a few percent of oxygen in the lattice.⁸ The ferromagnetic order is indicated by Fig. 4 which shows the spin polarization of the photoyield as a function of applied magnetic field. The polarization increases to $\sim 8\%$ and saturates above about 10 kOe. Such saturation is characteristic of a ferromagnet. The incorporated oxygen concentration in the surface of Fig. 4 was determined by Auger spectroscopy to be $3.3 \pm 0.5\%$. The saturation magnetization was found to increase with oxygen concentration. For the surface of Fig. 4, the polarization decreased nearly linearly with temperature over the measured range from 250 K to the transition temperature $T_c \approx 500$ K. Note that the Neel temperature for bulk antiferromagnetic Cr is $T_n = 310$ K. In contrast to these results for incorporated oxygen, when 0.6 monolayer was adsorbed on top of the surface, zero polarization was measured just as for the oxygen-free surface.

The oxygen which is incorporated in the lattice causes changes in the magnetic order of the Cr(100) surface way out of proportion to its concentration. Even if all the oxygen went to form the ferromagnetic compound Cr_2O , which is highly unlikely, the amount is an order of magnitude too low to produce the observed effects. A calculation of the unreconstructed Cr(100) surface³³ within a tight binding approximation shows that the enhanced density of states of the top-most layer is sufficient to fulfill the Stoner criterion suggesting that the Cr(100) surface is unstable to ferromagnetic order. Another calculation finds that surface spin fluctuations lead to large local moments at the surface which interact through itinerant bulk electrons and may order ferromagnetically.³⁴ Small amounts of oxygen in the Cr(100) surface appear able to tip the balance toward ferromagnetic order in a way not yet understood.

VI. REASONANT ENHANCEMENT OF THE Ni 6 eV SATELLITE

The satellite observed in photoemission spectra of the clean Ni surface at a binding energy of about 6 eV was found

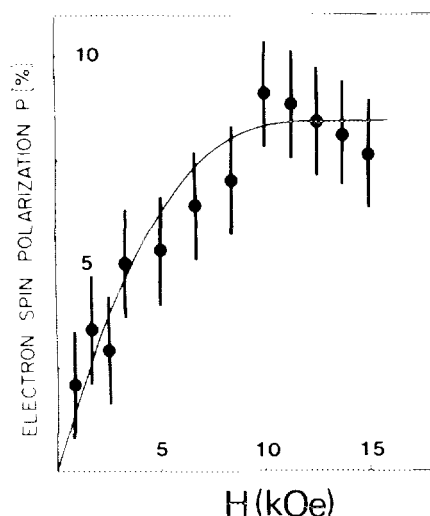


FIG. 4. The spin polarization of electrons photoemitted from Cr(100) with 3.3% oxygen incorporated is found to saturate as a function of magnetic field indicating magnetic order. From Meier *et al.* (Ref. 8).

by Guillot *et al.*³⁵ to exhibit a resonantlike enhancement at photon energies near the $3p \rightarrow 3d$ excitation energy of 67 eV. The discovery of this dramatic effect led to a flurry of experimental and theoretical investigations and a number of suggestions as to the origin of the resonant enhancement. Not only the enhancement, but the origin of the satellite itself and the recognition that it might be tied with the observed narrowing of the Ni d bands were causes of great interest.

The explanation that has come to be accepted is that the 6 eV satellite is due to a virtual bound state of two highly correlated d holes.^{36,37} The enhancement results from the increased probability of creating the two d -hole bound state by a $M_{2,3}M_{4,5}M_{4,5}$ Auger process. This process occurs over the narrow photon energy range where $3p_{3/2}$ and $3p_{1/2}$ electrons at binding energies of 66 and 67.6 eV, respectively, can be excited into the high density of unfilled d states which extend about 0.3 eV above the Fermi level of Ni.

Feldkamp and Davis³⁸ pointed out that the photoelectrons in the resonantly enhanced satellite peak should be spin polarized. The origin of the photoelectron spin polarization can be seen by reference to the inset of Fig. 5 without going to the details of their calculation. The unfilled $3d$ states are entirely of minority character $3d\downarrow$ so only a $3p\downarrow$ spin can be excited into such a state. Likewise, only a $3d\downarrow$ electron can

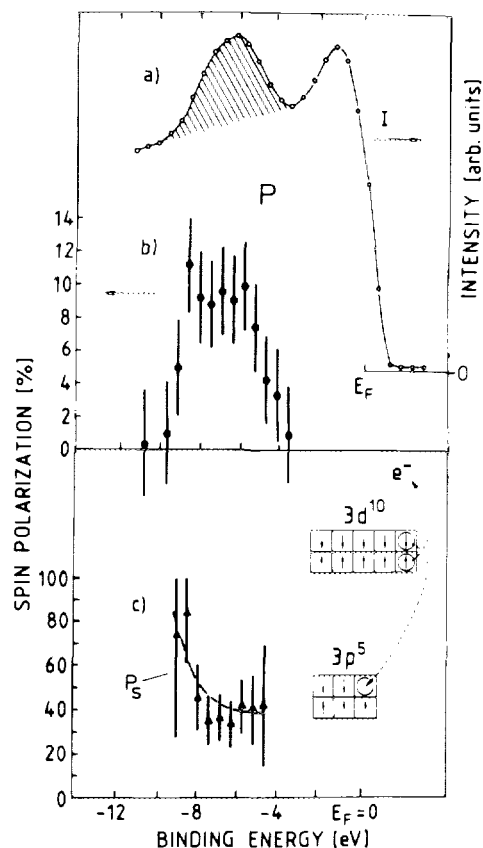


FIG. 5. (a) Photoelectron energy distribution curve of Ni(110) for $h\nu = 67.7$ eV. The shaded area is the 6 eV satellite. (b) The spin polarization of those photoelectrons of (a) with binding energies near the satellite. (c) Spin polarization of the satellite assuming an unpolarized background. Inset: A possible $M_{2,3}M_{4,5}M_{4,5}$ Auger process resulting in the emission of majority electron; $3p^63d^94s + h\nu \rightarrow 3p^63d^{10}4s \rightarrow 3p^63d^4s + e^-$. From Claiberg *et al.* (Ref. 9).

fall back into the $3p\downarrow$ hole; in general, either a $3d\uparrow$ or $3d\downarrow$ electron can be emitted. The $3d^8$ multiplet in Ni contains several components but the 1G dominates. For this singlet state, the spins of the d holes must be antiparallel requiring that only $3d\uparrow$ electrons are photoemitted to give 100% polarization. Feldkamp and Davis calculate the total polarization due to the contribution of all multiplet components and find $P = 60\%$. At photon energies above resonance where excitation of the $3p$ electron to $4s,p$ bands undergo ordinary Auger decay, no polarization is expected since the $4s,p$ bands are unpolarized and equal numbers of $3p\uparrow$ and $3p\downarrow$ holes are created. At most, a polarization reflecting the net spin density of the d electrons $\sim 5\%$ could be expected.

In an elegant experiment which involved the use of synchrotron radiation from the LURE storage ring and the first differential energy analysis along with polarization analysis, Clauberg *et al.*⁹ measured the polarization of the resonantly enhanced satellite photoelectrons. An energy distribution curve of photoelectrons from Ni(110) at $\hbar\omega = 67.7$ eV is shown in Fig. 5(a). The shaded region is the satellite peak. The measured polarization at the binding energy of the satellite is shown in Fig. 5(b). If this polarization is corrected for the contribution of the background under the shaded region, assuming the background to be unpolarized, the polarization for the satellite shown in Fig. 5(c) is obtained. As a function of photon energy, the satellite polarization increases abruptly at $\hbar\omega \approx 65$ eV, reaches a maximum of 50%–60% at $\hbar\omega = 67$ eV, and decreases at higher energy.

Even though these difficult resonant satellite polarization measurements have a large statistical uncertainty and some uncertainty in the background correction, they not only confirm the $M_{2,3}M_{4,5}M_{4,5}$ Auger enhancement mechanism of the two-hole satellite but also rule out a number of alternate mechanisms that have been proposed. For example, when a satellite structure which exhibited a resonant enhancement was found for Cu, a model involving a Fano-type resonance between two-electron excitations was proposed.³⁹ That model, as well as an additional model⁴⁰ involving a strong interaction between $4s$ and $4p$ conduction electrons with the two-hole bound state ($3d^8$ configuration) must not play an important role in Ni because neither would lead to a spin polarization. Similarly, a one-electron model where the satellite is thought to be an ordinary interband transition which is enhanced by final state effects in the joint density of states has been proposed.⁴¹ However, since the energy resolution of 1 eV in the polarized photoemission experiment does not allow separate measurement of spin up or spin down bands, the maximum polarization that can be observed in an interband transition is near the average valence band spin density of $\sim 5\%$ and therefore the interband transition explanation can be ruled out. Likewise, shake up structures where a d hole is created by excitation to a $4s$ or $4p$ state⁴² would not give a high polarization and therefore cannot be important.

VII. SPIN-POLARIZED INVERSE PHOTOELECTRON SPECTROSCOPY

In the preceding two sections results were presented from experiments in which the spin polarization of electrons emitted from occupied states below the Fermi level were mea-

sured. Here we discuss the complementary experiment that probes the spin dependent band structure of unfilled states above E_F . Earlier this year, it was shown that angle-resolved inverse photoelectron spectroscopy (IPES), or vacuum ultraviolet bremsstrahlung isochromat spectroscopy, could provide information on the dispersion of unfilled energy bands.⁴³

In the inverse photoelectron technique, the sample surface is bombarded with electrons and one measures the photon flux that is generated when these electrons undergo radiative transitions into unfilled states. A particularly suitable photon detector which has 0.7-eV bandpass centered at 9.7 eV⁴⁴ was used in these experiments. Spin-polarized IPES (SPIPES) was accomplished by replacing an ordinary electron gun with a GaAs-polarized electron source.¹⁷ The first measurements were made by Unguris *et al.*¹⁰ on a Ni(110) crystal which was ideal to test this new technique because of the high density of unfilled minority spin d states extending a few tenths of an eV above E_F .

The left panel of Fig. 6 shows a large peak in the photon flux N_\uparrow , corresponding to the spin polarization of the incident electron beam in the minority direction, which was observed at the Fermi level. The photon flux N_\downarrow due to incident electrons of the opposite spin direction has a smooth shape characteristic of a background due to electrons that are scattered inelastically in addition to undergoing a radiative transition. The lower part of the left panel shows the photon intensity asymmetry defined analogously to the scattered electron asymmetries discussed above $A = (N_\uparrow - N_\downarrow)/(N_\uparrow + N_\downarrow)$.

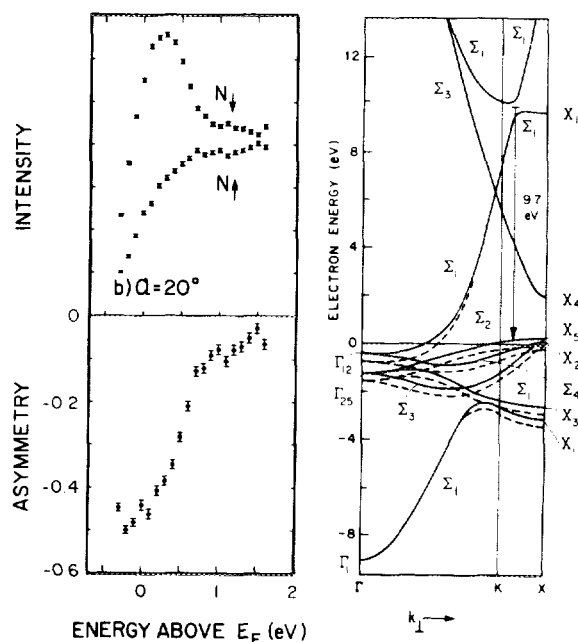


FIG. 6. Left panel: The photon intensity N_\uparrow and N_\downarrow due to transitions of majority and minority spin electrons to final states above E_F for an angle of incidence $\alpha = 20^\circ$. The asymmetry $A = (N_\uparrow - N_\downarrow)/(N_\uparrow + N_\downarrow)$ is shown in the lower part of the panel. Right panel: An energetically possible transition at $\hbar\omega = 9.7$ eV for electrons incident normally on Ni(110) is shown by the arrow in the band structure diagram. The dashed curves are majority spin bands. From Unguris *et al.* (Ref. 10).

The origin of the N_i peak is depicted by the $\hbar\omega = 9.7$ eV transition in the band structure diagram of Ni along the Γ KX direction shown in the right panel of Fig. 6. At normal incidence this transition is symmetry forbidden, which explains the observed increase in the peak size off normal incidence where the selection rule is relaxed.

This demonstration of angle-resolved SPIPES suggests further studies of the energy dispersion of d -hole states and studies of the changes in these states on chemisorption. Unguris *et al.*¹⁰ indicate potential for improving the count rate in their experiment and state that such experiments are no more technically demanding than spin-polarized photoemission.

VIII. CONCLUSION

Several examples where electron spin polarization measurements in surface studies have provided new insights have been described. New information can be gained both in nonmagnetic materials where the spin dependence is due to the spin-orbit interaction or in magnetic materials where the spin dependence due to the exchange interaction gives insight into surface magnetic behavior. The immense improvements in electron spin polarization sources and analyzers which have occurred in the past few years have greatly increased the practicality of electron spin polarization measurements. We believe the study of electron spin polarization phenomena to be an exciting new direction for surface science.

ACKNOWLEDGMENT

This work was supported in part by the Office of Naval Research.

¹D. T. Pierce and R. J. Celotta, *Adv. Electron. Electron Phys.* **56**, 219 (1981).

²S. F. Alvarado, W. Eib, F. Meier, H. C. Siegmann, and P. Zürcher, in *Photoemission and the Electronic Properties of Surface*, edited by B. Feuerbacher, B. Fitton, and R. F. Willis (Wiley, London, 1978) Chap. 18.

³P. J. Jennings and R. O. Jones, *Solid State Commun.* **44**, 17 (1982).

⁴R. O. Jones and P. J. Jennings *Phys. Rev. B* (to be published).

⁵S. F. Alvarado, M. Campagna, and H. Hopster, *Phys. Rev. Lett.* **48**, 51 1768 (1982); *Surf. Sci.* **117**, 294 (1982).

⁶S. F. Alvarado, M. Campagna, F. Ciccacci, and H. Hopster, *J. Appl. Phys.* (to be published).

⁷D. T. Pierce, R. J. Celotta, J. Unguris, and H. C. Siegmann, *Phys. Rev. B* **26**, 2566 (1982).

⁸F. Meier, D. Pescia, and T. Schriber, *Phys. Rev. Lett.* **48**, 645 (1982).

⁹R. Clauberg, W. Gudat, E. Kisker, E. Kuhlmann, and G. M. Rothberg, *Phys. Rev. Lett.* **47**, 1314 (1981).

¹⁰J. Unguris, A. Seiler, R. J. Celotta, D. T. Pierce, P. D. Johnson, and N. V. Smith, *Phys. Rev. Lett.* **48**, 1047 (1982).

¹¹D. Paraskevopoulos, R. Meservey, and P. M. Tedrow, *Phys. Rev. B* **16**, 4907 (1977).

¹²C. Rau and J. Eichner, *Phys. Rev. Lett.* **47**, 939 (1981).

¹³M. Landolt and M. Campagna, *Surf. Sci.* **70**, 197 (1978); M. Landolt, Y. Yafet, and B. Wilkins, *J. Appl. Phys.* **49**, 1418 (1978).

¹⁴J. Unguris, D. T. Pierce, A. Galejs, and R. J. Celotta, *Phys. Rev. Lett.* **49**, 72 (1982).

¹⁵G. Ravano, M. Erbudak, and H. C. Siegmann, *Phys. Rev. Lett.* **49**, 80 (1982).

¹⁶D. T. Pierce, F. Meier, and P. Zürcher, *Appl. Phys. Lett.* **26**, 670 (1975).

¹⁷D. T. Pierce, R. J. Celotta, G.-C. Wang, W. N. Unertl, A. Galejs, C. E. Kuyatt, and S. R. Mielczarek, *Rev. Sci. Instrum.* **51**, 478 (1980).

¹⁸B. Reihl, M. Erbudak, and D. M. Campbell, *Phys. Rev. B* **19**, 6358 (1979).

¹⁹F. Ciccacci, S. Alvarado, and S. Valeri, *J. Appl. Phys.* **53**, 4395 (1982).

²⁰J. Kirschner and R. Feder, *Phys. Rev. Lett.* **42**, 1008 (1979).

²¹H. C. Siegmann, D. T. Pierce, and R. J. Celotta, *Phys. Rev. Lett.* **46**, 452 (1981).

²²D. T. Pierce, S. M. Girvin, J. Unguris, and R. J. Celotta, *Rev. Sci. Instrum.* **52**, 1437 (1981).

²³M. Erbudak and G. Ravano, *J. Appl. Phys.* **52**, 5032 (1981).

²⁴P. J. Jennings, *Surf. Sci.* **75**, L773 (1978); **88**, L25 (1979).

²⁵E. G. McRae, *Rev. Mod. Phys.* **51**, 541 (1979).

²⁶R. E. Dietz, E. G. McRae, and R. L. Campbell, *Phys. Rev. Lett.* **45**, 1280 (1980).

²⁷J. C. LeBosse, J. Lopez, C. Gaubert, Y. Gauthier, and R. Baudoing, *J. Phys. C* **15**, 3425 (1982).

²⁸A. Adnot and J. D. Crette, *Phys. Rev. Lett.* **38**, 1084 (1977).

²⁹D. T. Pierce, R. J. Celotta, G.-C. Wang, and E. G. McRae, *Solid State Commun.* **39**, 1053 (1981); E. G. McRae, D. T. Pierce, G.-C. Wang, and R. J. Celotta, *Phys. Rev. B* **24**, 4230 (1981).

³⁰G. Malmström and J. Rundgren, *J. Phys. C* **14**, 4937 (1981).

³¹R. Feder and H. Pleyer, *Surf. Sci.* **117**, 285 (1982).

³²D. L. Mills and A. A. Maradudin, *J. Phys. Chem. Solids* **28**, 1885 (1967); D. L. Mills, *Comments Solid State Phys.* **4**, 28 (1971); **4**, 95 (1972). See also G. T. Rado, *Bull. Am. Phys. Soc. II* **2**, 127 (1957).

³³G. Allan, *Phys. Rev. B* **19**, 4774 (1979); *Surf. Sci.* **74**, 79 (1978).

³⁴D. R. Grempel, *Phys. Rev. B* **24**, 3928 (1981).

³⁵C. Guillot, Y. Ballu, J. Paigné, J. Lacante, K. P. Jain, P. Thiry, R. Pinchaux, Y. Pétroff, and L. M. Falicov, *Phys. Rev. Lett.* **39**, 1632 (1977).

³⁶D. R. Penn, *Phys. Rev. Lett.* **42**, 921 (1979).

³⁷A. Liebsch, *Phys. Rev. Lett.* **43**, 1431 (1979).

³⁸L. A. Feldkamp and L. C. Davis, *Phys. Rev. Lett.* **43**, 151 (1978).

³⁹M. Ivan, F. J. Himpsel, and D. E. Eastman, *Phys. Rev. Lett.* **43**, 1829 (1979).

⁴⁰L. C. Davis and L. A. Feldkamp, *Phys. Rev. Lett.* **44**, 673 (1980).

⁴¹J. Kanski, P. O. Nilsson, and C. G. Larsson, *Solid State Commun.* **35**, 397 (1980).

⁴²W. Eberhardt and E. W. Plummer, *Phys. Rev. B* **21**, 3245 (1980).

⁴³D. P. Woodruff and N. V. Smith, *Phys. Rev. Lett.* **48**, 283 (1982).

⁴⁴V. Dose, *Appl. Phys.* **14**, 117 (1977); G. Denninger, V. Dose, and H. Scheidt, *ibid.* **18**, 375 (1979).